JOURNAL OF SOLID STATE CHEMISTRY 97, 212–223 (1992)

Diffusion and Short-Range Order within the $Ba_{1-x}Bi_xF_{2+x}$ ($0 \leq x \leq 0.45$) Solid Solution Quenched from 700°C

SUH KYUNG SOO, J. SÉNÉGAS, J. M. RÉAU, M. WAHBI, AND P. HAGENMULLER

Laboratoire de Chimie du Solide du CNRS, Université de Bordeaux I, 351 cours de la Libération, 33405 Talence Cedex, France

Received March 22, 1991; in revised form September 24, 1991

An investigation of the fluorite-type $Ba_{1-x}Bi_xF_{2+x}$ ($0 \leq x \leq 0.45$) solid solution has been carried out by conductivity measurements and by ^{19}F NMR on samples quenched from 700°C. Application of the "clustering process" model to $Ba_{1-x}Bi_xF_{2+x}$, which involves a conductivity maximum for $x_{max.} \cong 0.35$, has allowed us to propose a progressive transformation within the solid solution of 4 : 4 : 3 clusters into 8 : 12 : 1 clusters as x increases. Interpretation of the NMR results is based on the existence of different fluoride ion sublattices and partial exchange between them at increasing temperature. A diffusive character of the F^- ion motion is ascertained above $T \simeq 320$ K by comparing the activation energies determined by NMR and conductivity measurements. The NMR study confirms the validity of the clustering process proposed for $Ba_{1-x}Bi_xF_{2+x}$ and illustrates the difference in the electrical behavior of interstitial fluoride ions belonging to the 4 : 4 : 3 and 8 : 21 : 1 clusters.

I. Introduction

Different criteria characterizing the high mobility of the F^- ions in the $M^{2+}_{1-x}M'^{2+\alpha}_{x}F_{2+\alpha x}$ (α = 1,2,3) solid solutions with fluorite-type structure has been pointed out in some exhaustive investigations (*1*, *2*): vacancies in the normal anionic sublattice, high polarizability of the cations, significant size difference between the various types of cations involved etc. They have allowed us to isolate a large number of very fast ionic conductors such as $Pb_{0.75}Bi_{0.25}F_{2.25}$ (*3*), $ABiF_4$ (A = K,Rb,Tl) (*4*), $PbSnF_4$ (*5*), etc. These starting criteria are also responsible for the establishment of a short-range order in the apparently disordered solid solutions; the resulting transport properties depend closely on the type of clustering and its extension at increasing substitution rate. Recently we have proposed a model relating in a continuous manner the composition dependence of the electrical properties and the progressive extension of the clustering with increasing x in the $M^{2+}_{1-x}M'^{2+\alpha}_{x}F_{2+\alpha x}$ solid solutions (*6*, *7*).

The application of this clustering process model to various solid solutions has allowed us to determine the nature of the clusters set up in the materials. These extended defects appearing for $x \gtrsim 0.01$ are labelled $n_1 : n_2 : n_3$ and based on the association of n_1 vacancies in the normal positions of the fluorite-type network, n_2 F′ ($\frac{1}{2}$,u,u) and n_3 F″ (v,v,v) interstitial anions (*8*). So the existence of the n + 1 : $2n$: 1 single-file monodimensional clusters, of the $2n$ + 2 : $3n$: 2 and $2n$ + 2 : $4n$: 2 two-file ones, the length of which

0022-4596/92 $3.00

grows when x increases, has been established respectively for $Pb_{1-x}Bi_xF_{2+x}$, $Pb_{1-x}In_xF_{2+x}$, and $Pb_{1-x}Zr_xF_{2+2x}$ (*9*). The $Ca_{1-x}Ln_xF_{2+x}$ series is characterized either by presence of 1 : 0 : 3 clusters when Ln^{3+} is a large size cation (*10*) or by progressive transformation with rising x of 4 : 4 : 3 clusters into cubooctahedral 8 : 12 : 1 clusters when it is a small size cation, e.g., Lu^{3+} (*11*). The validity of the short-range models proposed for the solid solutions has been confirmed by the good fitting between the calculated numbers of vacancies and of interstitial anions and those experimentally determined by ^{19}F NMR or neutron diffraction.

Our investigations have been extended to the fluorite-type $Ba_{1-x}Bi_xF_{2+x}$ ($0 \leq x \lesssim 0.45$) solid solution (*12*): we aimed at determining the clustering process from the composition dependence of the F^- ion conductivity. A ^{19}F NMR study and a neutron diffraction investigation have been simultaneously carried out for several compositions to check the validity of the short-range order model proposed for $Ba_{1-x}Bi_xF_{2+x}$.

This paper collects the results obtained from conductivity measurements and ^{19}F NMR studies achieved on samples obtained in similar experimental conditions. Valuable information relative to the existence of various possible sites for the F^- ions and to the diffusion of mobile fluoride ions could be expected from the NMR investigation and confronted with the anionic conduction properties.

II. Reminder of the Properties of the Phases Belonging to the BaF_2–BiF_3 System

XRD analysis of the BaF_2–BiF_3 system after synthesis from the binary fluorides at 700°C in sealed gold tubes and quenching from that temperature had allowed us to detect (*12*)

(i) for $0 \leq x \lesssim 0.45$, a disordered cubic symmetry solid solution of composition $Ba_{1-x}Bi_xF_{2+x}$; its structure is of the fluorite-type.

(ii) for $0.45 \lesssim x \lesssim 0.50$, an ordered solid solution of composition $Ba_{1-x}Bi_xF_{2+x}$ whose structure derives from the fluorite-type.

(iii) for $0.83 \leq x \leq 0.95$, a disordered hexagonal solid solution of the tysonite-type.

III. Electrical Properties of the $Ba_{1-x}Bi_xF_{2+x}$ ($0 \leq x \lesssim 0.45$) Solid Solution Quenched from 700°C

Conductivity measurements have been carried out on powder samples pressed to form pellets, sintered at 700°C in large sealed gold tubes, and then quenched. The compactness of the pellets was about 90%. Vacuum evaporated gold was used as electrodes. The bulk resistance was measured by the complex impedance method using a Solartron frequency response analyzer (*13*). The frequency range was 10^{-2}–10^4 Hz; measurements were carried out for several temperature cycles between 20 and 250°C.

In this temperature range, for all samples investigated, the temperature dependence of the conductivity is in agreement with an Arrhenius-type law.

Figure 1 gives, for instance, the conductivity isotherm at $T = 400$ K and the variation of the activation energy ΔE_σ as a function of substitution rate for the $Ba_{1-x}Bi_xF_{2+x}$ solid solution quenched from 700°C: a maximum of $\log \sigma_{400\,K}$ associated with a minimum of ΔE_σ appears clearly for $x_{max.} \simeq 0.35$.

There is a large analogy between the composition dependences of the electrical properties of the disordered $Ca_{1-x}Y_xF_{2+x}$ ($0 \leq x \leq 0.38$) (*11*) and $Ba_{1-x}Bi_xF_{2+x}$ ($0 \leq x \lesssim 0.45$) solid solutions. On the other hand, the existence of cubooctahedral 8 : 12 : 1 clusters has been shown as well in the $Ca_{14}Y_5F_{43}$ tveïtite (*14*) as in the related ordered $Ba_{1-x}Bi_xF_{2+x}$ ($0.45 \lesssim x \lesssim 0.50$) phase (*12*). These results have incited us to propose for Ba_{1-x}

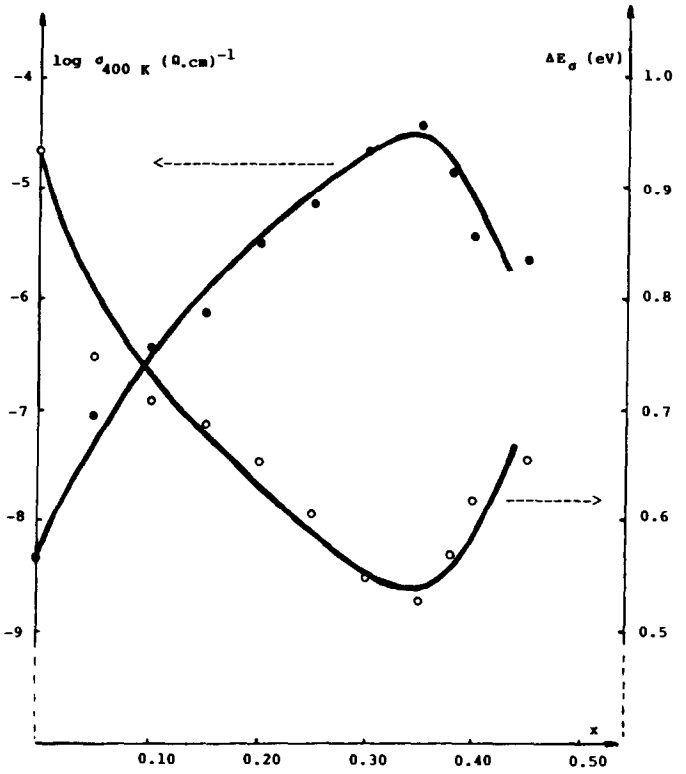

FIG. 1. Composition dependence of log $\sigma_{400\,K}$ and ΔE_σ for the $Ba_{1-x}Bi_xF_{2+x}$ solid solution quenched from 700°C.

Bi_xF_{2+x} ($0 \leq x \lesssim 0.45$) the same clustering process as that previously detected for $Ca_{1-x}Y_xF_{2+x}$, i.e., a progressive transformation of 4 : 4 : 3 clusters into 8 : 12 : 1 ones as x increases.

IV. Proposition of a Clustering Process in $Ba_{1-x}Bi_xF_{2+x}$ ($0 \leq x \lesssim 0.45$)

The clustering process model allows us to correlate the composition dependence of the electrical properties and the progressive clustering extension when x increases in the fluoride anion excess CaF_2-type solid solutions of $M^{2+}_{1-x}M'^{2+\alpha}_{x}F_{2+\alpha x}$ ($\alpha = 1,2,3$) formulation (7). According to this model the sum of interstitial fluoride ions and the amount of vacancies in normal sites are respectively represented by the functions $(y_{int.})_{tot.}$ and $(y_\square)_{tot.}$ which depend on three parameters called λ, m, and x_s:

$$(y_{int.})_{tot.} = \frac{mx^3 + \lambda x_s^2 x}{x^2 + x_s^2}$$

$$(y_\square)_{tot.} = \frac{(m-\alpha)x^3 + (\lambda - \alpha)x_s^2 x}{x^2 + x_s^2}.$$

The λ and m parameters define respectively the clustering conditions for the lowest and highest values of x; x_s is bound with electrical properties: its value is close to $x_{max.}$, substitution rate for which a conductivity maximum can be observed in the composition dependence of conductivity (7).

The presence in $Ba_{1-x}Bi_xF_{2+x}$ of a conductivity maximum for $x_{max.} \simeq 0.35$ and the hypothesis of a progressive transformation of 4 : 4 : 3 clusters into 8 : 12 : 1 clusters as x

increases result in a precise determination of the λ, m, and x_s parameters for that solid solution:

$$\lambda = 7/3;\ m = 13/5;\ x_s = 1/2\sqrt{2} \simeq 0.353.$$

Table I gives the analytical expressions representing $(y_{int.})_{tot.}$, $(y_{\square})_{tot.}$, $(y_{F'})_{tot.}$ and $(y_{F''})_{tot.}$, and their respectively calculated values for $x = 0.20, 0.30$, and 0.40. We have included in Table I the values of $y_{int.}$, $y_{\square}$, $y_{F'}$, and $y_{F''}$ relative to 4 : 4 : 3 and 8 : 12 : 1 clusters.

V. ^{19}NMR Investigation of the $Ba_{1-x}Bi_xF_{2+x}$ ($0 < x \lesssim 0.45$) Solid Solution Quenched from 700°C

The samples correspond to various substitution rates (x = 0.10, 0.20, 0.30, and 0.40) of the $Ba_{1-x}Bi_xF_{2+x}$ solid solution quenched from 700°C. They have been prepared in the same experimental conditions as those used for electrical measurements.

TABLE I

ANALYTICAL EXPRESSIONS OF $(y_{int.})_{tot.}$, $(y_{\square})_{tot.}$, $(y_{F'})_{tot.}$, AND $(y_{F''})_{tot.}$ FOR $Ba_{1-x}Bi_xF_{2+x}$ QUENCHED FROM 700°C AND VALUES OF FUNCTIONS RELATIVE TO 4 : 4 : 3 AND 8 : 12 : 1 CLUSTERS CALCULATED FOR x = 0.20, 0.30, and 0.40.

x	0.20	0.30	0.40
$(y_{int.})_{tot.}$	0.479	0.733	0.993
$(y_{\square})_{tot.}$	0.279	0.433	0.593
$(y_{F'})_{tot.}$	0.318	0.534	0.773
$(y_{F''})_{tot.}$	0.161	0.199	0.220
$(y_{int.})_{4:4:3}$	0.353	0.407	0.409
$(y_{\square})_{4:4:3}$	0.202	0.232	0.234
$(y_{F'})_{4:4:3}$	0.202	0.233	0.234
$(y_{F''})_{4:4:3}$	0.151	0.174	0.175
$(y_{int.})_{8:12:1}$	0.126	0.326	0.584
$(y_{\square})_{8:12:1}$	0.077	0.201	0.359
$(y_{F'})_{8:12:1}$	0.116	0.301	0.539
$(y_{F''})_{8:12:1}$	0.010	0.025	0.045

Note.

$$(y_{int.})_{tot.} = \frac{x(312x^2 + 35)}{15(8x^2 + 1)};\quad (y_{\square})_{tot.} = \frac{x(192x^2 + 20)}{15(8x^2 + 1)}$$

$$(y_{F'})_{tot.} = \frac{x(288x^2 + 20)}{15(8x^2 + 1)};\quad (y_{F''})_{tot.} = \frac{x(24x^2 + 15)}{15(8x^2 + 1)}.$$

V-1. Experimental—High Resolution Solid State NMR

NMR experiments were performed on a Bruker MSL-200 spectrometer (B_0 = 4.7 T) equipped with a standard variable temperature unit in the temperature range −150 to 150°C.

A "one pulse" sequence program has been used instead of the "Hahn-echo" sequence that is generally used for the ($I = \frac{1}{2}$) nuclei in solids. The reasons of this substitution are the following:

—The fluoride anions in the investigated samples have different diffusion coefficients.

—The "one pulse" program which uses a very short $\pi/2$ pulse length time (0.61 μs) allowed us to obtain a large domain of the flat central portion in the power irradiation spectrum.

The spectrometer operating conditions have been the following:

—Spectrometer frequency: 188.283 MHz.

—Pulse program: 90° pulse width, 0.7 μs; dead time delay (ringdown delay), 6 μs; recycle delay time, 10 s.

Simulations of the ^{19}F NMR lines were performed using the "LINESIM" program provided by Bruker. This program allows adjusting peak position, peak height, line width, ratio of Gaussian and Lorentzian functions, and relative proportions of their areas.

When a single Gaussian cannot fit exactly with the registered spectrum, an appropriate mixing of Gaussian and Lorentzian functions is used for the simulation. It is the case, in particular, for the spectra concerning the motional narrowing temperature range.

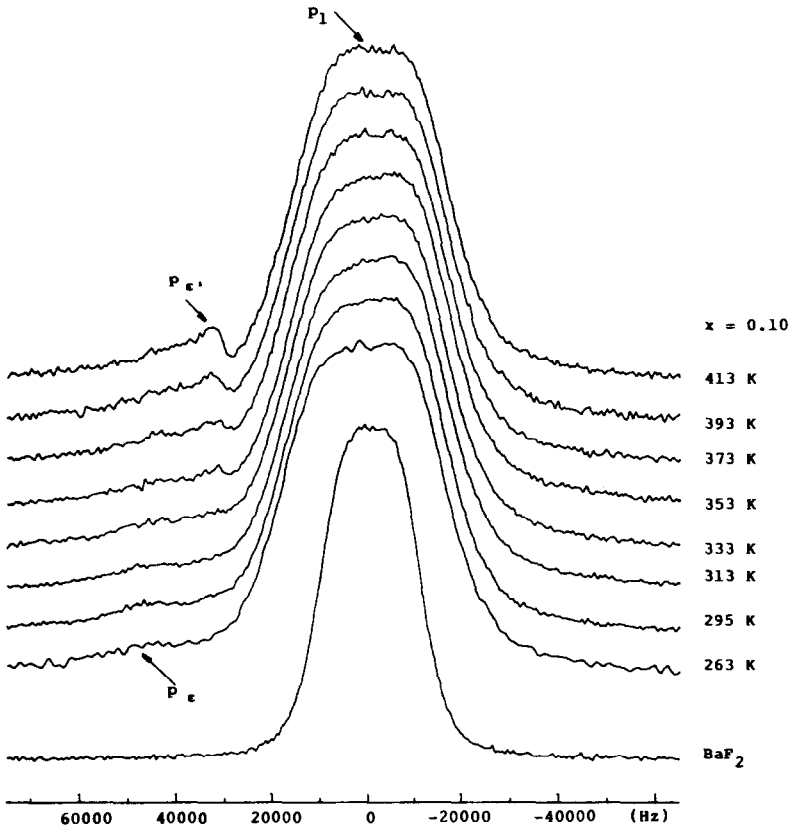

FIG. 2. ^{19}F NMR spectrum for pure BaF_2 at 295 K and for the $Ba_{0.90}Bi_{0.10}F_{2.10}$ sample at different temperatures.

V-2. Results

V-2-1. The $Ba_{0.90}Bi_{0.10}F_{2.10}$ composition. The ^{19}F NMR spectrum is given for various temperatures in Fig. 2 for $Ba_{0.90}Bi_{0.10}F_{2.10}$. A large peak, called p_1, is shown, the thermal variation of which is very weak in the temperature range considered (263–413 K). The relative variation of the second moment (M_2) in the spectra recorded at 263 and 413 K is only 3%.

Whatever the temperature, the fullwidth at half-height (FWHH) of the spectrum observed for $Ba_{0.90}Bi_{0.10}F_{2.10}$ is significantly larger ($\simeq$35 KHz) than that of BaF_2 ($\simeq$22 KHz) (Fig. 2). This line broadening can be attributed to Bi^{3+}–F^- dipolar interactions in $Ba_{0.90}Bi_{0.10}F_{2.10}$.

The p_1 peak is large enough to be considered as the sum of two lines, one corresponding to fluoride ions located in normal positions of the CaF_2-type structure and the other to anions slightly relaxed from those positions.

On the other hand, in the high frequency domain a small peak, called p_ε, can be observed at low temperature (Fig. 2); it disappears at rising temperature but is replaced by another small peak, $p_{\varepsilon'}$. Attributing both peaks to particular fluoride ion positions is difficult, all the more as their contribution to the total line is very small ($\simeq$1 to 2% for

p_ε at 263 K and ≈2 to 3% for $p_{\varepsilon'}$ at 413 K). They could be interpreted as fluoride ions constituting respectively *nn* and *nnn* pairs (*15, 16*). Indeed these tiny peaks are missing in the spectra obtained for materials corresponding to higher substitution rates, i.e., belonging to a composition domain where well organized clusters appear. The investigation of samples corresponding to $x < 0.10$, for which the contribution of p_ε and $p_{\varepsilon'}$ ought to be larger, will permit confirmation of our hypothesis.

V-2-2. The $Ba_{1-x}Bi_xF_{2+x}$ compositions (x = 0.20, 0.30, and 0.40). Figure 3 gives, for example, the ^{19}F spectrum at different temperatures for the $Ba_{0.70}Bi_{0.30}F_{2.30}$ composition. Analogous results have been obtained for x = 0.20 and 0.40.

Two peaks, called p_1 and p_2, are shown at very low temperatures ($T < 200$ K) and can be attributed, whatever the value of x, to fluoride ions localized respectively in normal sites of the fluorite-type lattice and outside of those positions; their contribution is temperature independent, which means that all F^- ions present are fixed in the NMR time scale in this temperature domain.

Above a T_1 temperature, a new peak, called p_m, located between the p_1 and p_2 peaks can be observed. It is growing with the temperature and it represents the fluoride ions which are mobile above T_1.

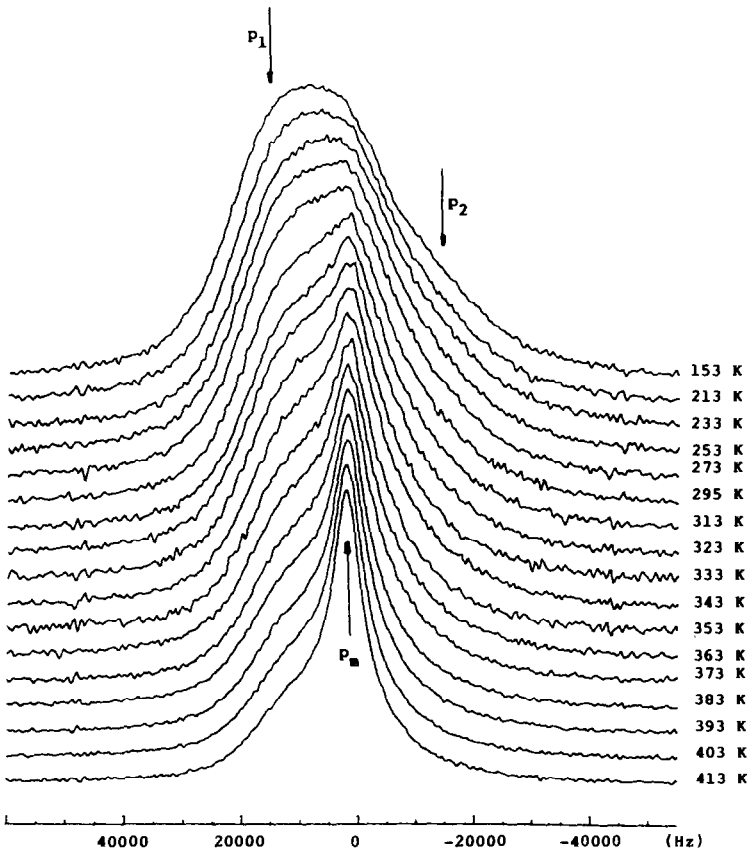

FIG. 3. Thermal variation of the ^{19}F NMR spectrum for the $Ba_{0.70}Bi_{0.30}F_{2.30}$ composition.

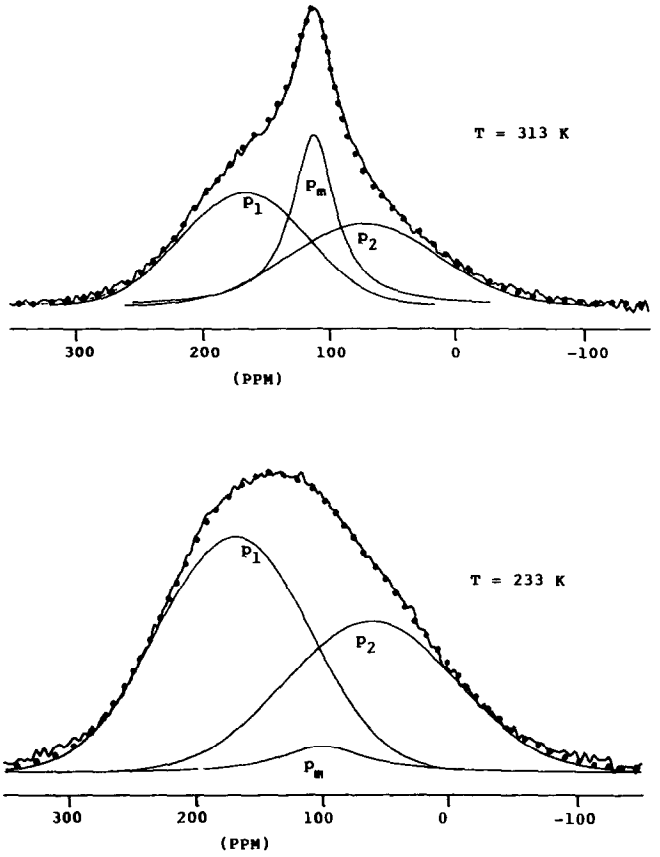

FIG. 4. Deconvolution of the ^{19}F NMR spectrum at 233 and 313 K for $Ba_{0.70}Bi_{0.30}F_{2.30}$.

The relative contributions of the three peaks observed at each temperature are determined by deconvolution of the whole spectrum. Figure 4 gives, as an example, the deconvolution of the ^{19}F NMR spectrum at 223 and 313 K for the $Ba_{0.70}Bi_{0.30}F_{2.30}$ composition: the fluoride ions rates considered as proportional to the areas of the p_1, p_2, and p_m peaks can be so determined for each temperature used. The temperature dependence of those rates is given respectively in Fig. 5a and Fig. 5b for $x = 0.20$ and $x = 0.30$.

Above T_1, p_2 and p_m merge progressively at rising temperature (Fig. 3); this phenomenon results from an increase of the number of mobile fluoride ions and from a simultaneous decrease of the amount of non mobile fluoride ions of p_2 type (Fig. 5).

Above a new temperature T_2 ($T_2 > T_1$), p_1 coalesces in turn with p_m when the temperature increases (Fig. 3). It means that the number of mobile fluoride ions increases now quickly not only to the detriment of the fluoride ions of p_2 type, but especially to that of F^- ions of p_1 type.

Above a T_3 temperature ($T_3 > T_2$), the number of the fixed fluoride ions of p_2 type becomes almost constant and temperature independent up to the highest experimental temperature considered (413 K); this

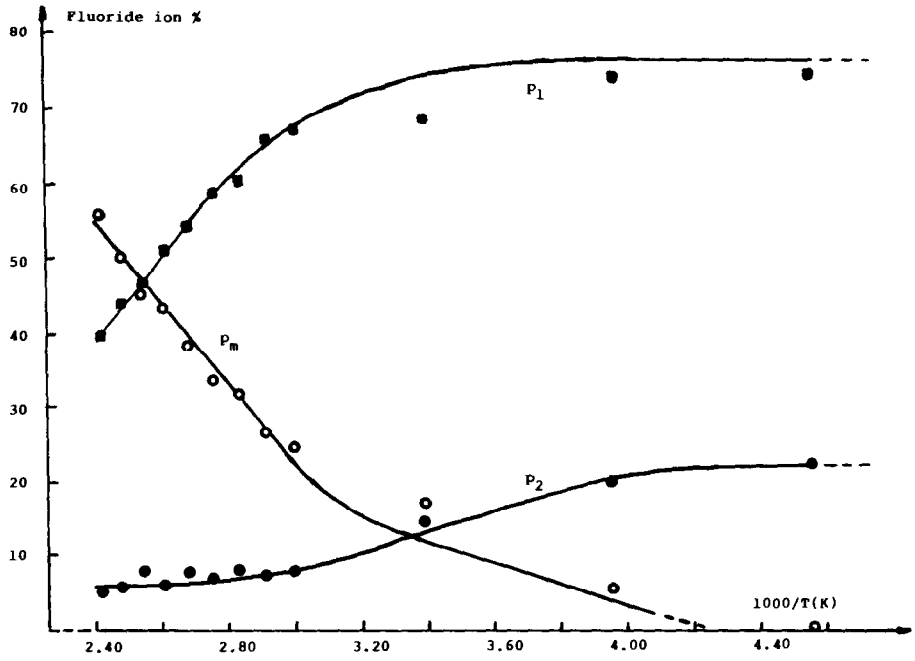

FIG. 5a. Temperature dependence of the fluoride ion rates assumed to be proportional to the p_1, p_2, and p_m peak areas for $Ba_{0.80}Bi_{0.20}F_{2.20}$.

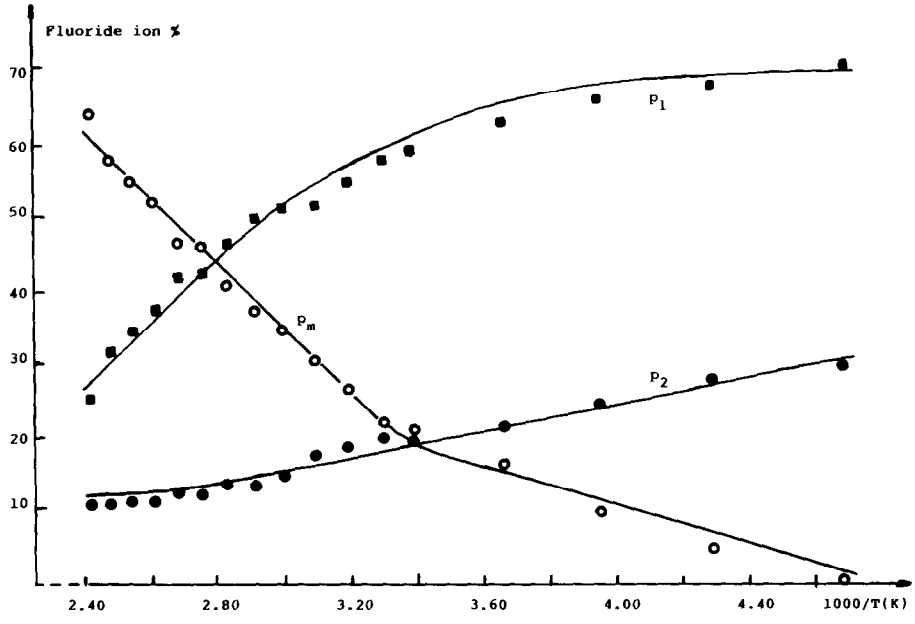

FIG. 5b. Temperature dependence of the fluoride ion rates assumed to be proportional to the p_1, p_2, and p_m peak areas for $Ba_{0.70}Bi_{0.30}F_{2.30}$.

TABLE II

VALUES OF T_1, T_2, AND T_3 TEMPERATURES FOR THE $Ba_{1-x}Bi_xF_{2+x}$ COMPOSITIONS RELATIVE TO $x = 0.20$, 0.30, AND 0.40

x	0.20	0.30	0.40
T_1	≃240 K	≃210 K	≃240 K
T_2	≃290 K	≃260 K	≃320 K
T_3	≃350 K	≃350 K	≃370 K

TABLE III

RATES OF FLUORIDE IONS NON-MOBILE IN THE TEMPERATURE DOMAINS CONSIDERED AND LOCALIZED IN NORMAL ($F_{norm.}$) OR INTERSTITIAL ($F_{int.}$) SITES

x	0.20	0.30	0.40
	Low temperature ($T < T_1$)		
$(p_1)_{lim.}$	77%	69%	60%
$(p_2)_{lim.}$	23%	31%	40%
	High temperature ($T_3 < T < 413$ K)		
$(p_2)_{lim.}$	6%	12%	20%
	Clustering model		
$(y_{int.})_{tot.}$	21.77%	31.87%	41.37%
$(y_{norm.})_{tot.}$	78.23%	68.13%	58.63%
$(y_{int.})_{443}$	16.04%	17.70%	17.04%
$(y_{int.})_{8\underline{12}1}$	5.73%	14.17%	24.33%

amount of p_2-type fixed F^- ions increases with x (Fig. 5).

The T_1, T_2, and T_3 temperatures, given in Table II cannot be determined with high accuracy. Nevertheless, it appears clearly that T_1 and T_2 are slightly lower for $x = 0.30$ than for $x = 0.20$ and 0.40.

VI. Diffusion and Clustering in the $Ba_{1-x}Bi_xF_{2+x}$ Solid Solution

The ^{19}F NMR study for the $Ba_{1-x}Bi_xF_{2+x}$ compositions corresponding to high values of x ($x \gtrsim 0.20$) has allowed us to show two exchange mechanisms between fluoride sublattices which occur progressively at increasing temperature.

The temperature dependence of p_2 (Fig. 5), which represents the fixed anion rate for the F^- ions located outside the normal sites, shows the existence of two groups of interstitial F^- ions: those which are mobile above T_1 and those which are not yet mobile above T_3 and are even fixed at 400 K.

By extrapolation of p_1 at low temperature and of p_2 at low and high temperatures, the lower and upper limit rates of fixed fluoride ions at low and high temperatures can be deduced and compared in Table III to those calculated from the model (Table I). Whatever the value of x:

at low temperature ($T < T_1$): $(F_{norm.})_{lim} \simeq (y_{norm.})_{tot.} = 2 - (y_{\square})_{tot.}$

$(F_{int.})_{lim} \simeq (y_{int.})_{tot.}$

at high temperature ($T_3 < T < 413$ K): $(F_{int.})_{lim} \simeq (y_{int.})_{8:12:1}$

Hence the ^{19}F NMR investigation of $Ba_{1-x}Bi_xF_{2+x}$ confirms the validity of the clustering process proposed from the model for that solid solution. Furthermore, it has shown that in the considered temperature domain the first fluoride ions mobile at low temperature are the interstitial anions belonging to the 4 : 4 : 3 clusters. At higher temperature in turns the anions located in the normal positions become mobile, but the interstitial fluoride ions belonging to the 8 : 12 : 1 clusters do not seem participate in

the conductivity mechanism in the temperature domain concerned by the measurements.

VII. Comparison of the Activation Energies Deduced from NMR and Conductivity Measurements

The activation energy of the mobile F^- ion relaxation for the $x = 0.20$, 0.30, and 0.40 compositions has been determined from the thermal variation of the jump frequency.

Line narrowing occurs when the fluorine jump frequency ν_s is of the same order of magnitude as the rigid lattice linewidth value. The thermal variation of ν_s can be deduced, as usual (*17*), from that of $\Delta\nu_{1/2}$, half-width measured at T temperature.

The determination of $\Delta\nu_{1/2}$ is difficult to achieve in the temperature domain investigated due to partial overlapping of p_m and p_2 lines and then of p_m, p_2, and p_1. Consequently, the jump frequency ν_s has been determined only in the high temperature domain, i.e., above 320 K.

Figure 6 shows the variation of log ν_s vs $10^3\ T^{-1}$ for $x = 0.20$, 0.30, and 0.40. An activation energy ΔE_F can be deduced for each sample.

In the high temperature domain considered where the anionic motions are enhanced by the increasing temperature, they contribute to a relaxation which is thermally activated. In the temperature range where relaxation results simultaneously from the atomic and spin diffusion, the measured activation energy represents $\frac{3}{4}$ of the activation energy of the atomic motions (*18*, *19*). Hence the activation energy of the mobile fluorine ions (p_m sublattice) is $\Delta E_1 = (\frac{4}{3})\ \Delta E_F$. The values of ΔE_1 are given for $x = 0.20$, 0.30, and 0.40 in Table IV.

At a given temperature the jump fre-

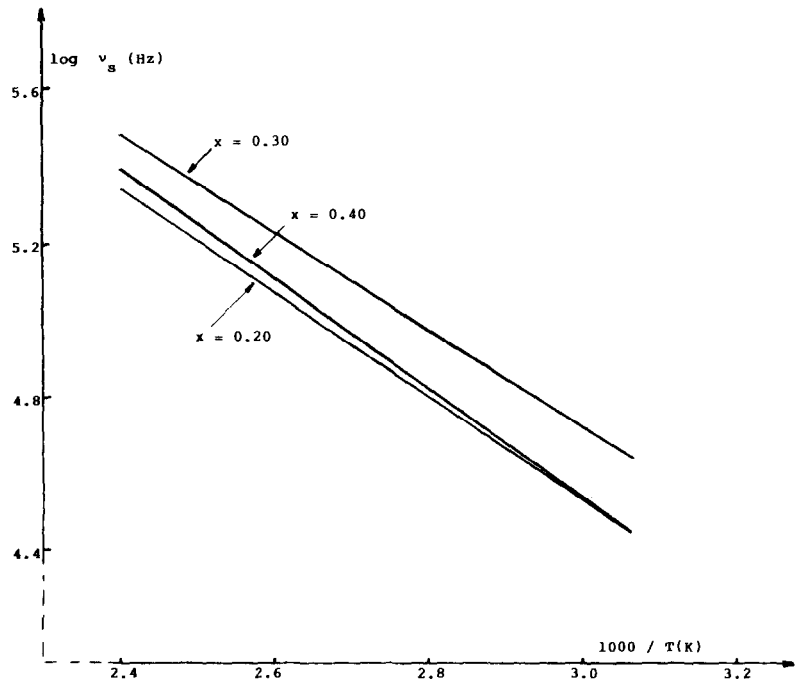

FIG. 6. Variation of log ν_s vs 10^3T^{-1} for $x = 0.20$, 0.30, and 0.40.

quency ν_s in the temperature range 320–413 K is higher for $x = 0.30$ than for $x = 0.20$ and 0.40 (Fig. 6). On the other hand, a lower value of ΔE_1 is observed for $x = 0.30$ (Table IV). Those results are in agreement with the composition dependence of the electrical properties (Fig. 1).

The temperature dependence of p_m in this temperature range is thermally activated and corresponds to an Arrhenius-type law (Fig. 5). The values of ΔE_2 are given for $x = 0.20$, 0.30, and 0.40 in Table IV: the $x = 0.30$ substitution rate leads to a lower value of ΔE_2 than $x = 0.20$ and 0.40, in agreement with the composition dependence of transport properties (Fig. 1).

Table IV allows one to compare the activation energies ΔE_t ($\Delta E_t = \Delta E_1 + \Delta E_2$) deduced from the NMR investigations and ΔE_σ determined from the conductivity measurements; for each value of x, a good agreement is observed between ΔE_t and ΔE_σ. Such a result shows clearly the diffusive character of F ion motions.

Furthermore the NMR investigation confirms the existence of a conductivity maximum connected to an activation energy minimum in the composition dependence of electrical properties. The $x = 0.30$ sample is characterized by a larger carrier mobility and a lower distribution width of the activation energies, with respect to the $x = 0.20$ and $x = 0.40$ compositions.

TABLE IV

COMPARISON OF THE ACTIVATION ENERGIES DEDUCED FROM THE NMR AND CONDUCTIVITY MEASUREMENTS

x	0.20	0.30	0.40
ΔE_1 (ev)	0.36	0.33	0.38
ΔE_2 (eV)	0.24	0.20	0.25
ΔE_t (eV) ($\Delta E_t = \Delta E_1 + \Delta E_2$)	0.60	0.53	0.63
ΔE_σ (eV)	0.65	0.55	0.62

VIII. Conclusions

The investigation of the composition dependence of the transport properties of the $Ba_{1-x}Bi_xF_{2+x}$ ($0 \leq x \lesssim 0.45$) solid solution quenched from 700°C has given evidence of a conductivity maximum associated with an activation energy minimum for $x_{max.} \simeq 0.35$. A clustering process has been proposed for $Ba_{1-x}Bi_xF_{2+x}$: it consists in a progressive transformation of 4:4:3 clusters into 8:12:1 clusters as x increases.

The NMR study has shown the existence of two F^- ion sublattices, the first representing the normal sites of the fluorite-type structure, the second the interstitial sites. Two subgroups of interstitial anions belonging to 4:4:3 and 8:12:1 clusters have actually been identified by an electrical behavior which differs with rising temperature. In the temperatutre domain concerned, the first anions which are mobile at low temperature are the interstitial anions belonging to 4:4:3 clusters, the F^- ions occupying the normal positions become only mobile at higher temperature; on the contrary, the interstitial anions of the 8:12:1 cubooctahedral clusters do not participate as mobile ions in the conductivity mechanism.

References

1. J. M. RÉAU, *in* "Materials for Solid State Batteries" (B. V. R. Chowdari and S. Radhakrishna, Eds.), pp. 193–208, World Scientific, Singapore (1986).
2. J. M. RÉAU AND J. GRANNEC, *in* "Inorganic Solid Fluorides, Chemistry and Physics" (P. Hagenmuller, Ed.), pp. 423–467, Academic Press, New York (1985).
3. C. LUCAT, G. CAMPET, J. CLAVERIE, J. PORTIER, J. M. RÉAU, AND P. HAGENMULLER, *Mater. Res. Bull.* **11**, 167 (1976).
4. C. LUCAT, PH. SORBE, J. PORTIER, J. M. RÉAU, P. HAGENMULLER, AND J. GRANNEC, *Mater. Res. Bull.* **12**, 145 (1977).
5. C. LUCAT, A. RHANDOUR, J. M. RÉAU, J. PORTIER, AND P. HAGENMULLER, *J. Solid State Chem.* **29**, 373 (1979).
6. J. M. RÉAU AND P. HAGENMULLER, *Appl. Phys.* **A49**, 3 (1989).

7. J. M. RÉAU, M. WAHBI, J. SÉNÉGAS, AND P. HAGENMULLER, "Proceedings, ICAM 91/EMRS 1991, Conf. A2-V8, Strasbourg, 1991."
8. A. K. CHEETHAM, B. E. F. FENDER, B. STEELE, R. I. TAYLOR, AND B. T. M. WILLIS, *Solid State Commun.* **8,** 171 (1970).
9. J. M. RÉAU, M. EL OMARI, J. SÉNÉGAS, AND P. HAGENMULLER, *Solid State Ionics,* **38,** 123 (1990).
10. M. EL OMARI, J. M. RÉAU, J. SÉNÉGAS, J. P. LAVAL, AND B. FRIT, *J. Fluorine Chem.* (1991), in press.
11. M. EL OMARI, J. M. RÉAU, AND J. SÉNÉGAS, *J. Solid State Chem.* **87,** 430 (1990).
12. J. M. RÉAU, TIAN SHUN BAO, A. RHANDOUR, S. MATAR, AND P. HAGENMULLER, *Solid State Ionics* **15,** 217 (1985).
13. J. F. BAUERLE, *J. Phys. Chem.* **30,** 2657 (1969).
14. D. J. M. BEVAN, O. GREIS, AND J. STRÂHLE, *Acta Crystallogr., Sect. A: Cryst. Phys. Diffr. Theor. Gen. Crystallogr.* **32,** 889 (1980).
15. H. W. DEN HARTOG, K. F. PEN, AND J. MEULDIJK, *Phys. Rev. B* **28,** 6031 (1983).
16. J. MEULDIJK AND H. W. DEN HARTOG, *Phys. Rev. B* **28,** 1036 (1983).
17. N. BLOEMBERGEN, E. M. PURCELL, AND R. V. POUND, *Phys. Rev.* **73,** 679 (1948).
18. Y. ROINEL AND J. P. WINTER, *J. Phys.* **31,** 351 (1970).
19. T. R. PHUA, B. J. BEAUDRY, D. T. PETERSON, J. R. TORGESON, R. G. BARNES, M. BELHOUL, G. A. STYLES, AND E. F. W. SEYMOUR, *Phys. Rev. B* **28** 6227 (1983).